# The study of a defect evolution in iron under fatigue loading in gigacyclic fatigue regime

O. Plekhov (http://orcid.org/0000-0002-0378-8249)
O. Naimark
*Institute of Continuous Media Mechanics UB RAS, 614014 Perm, Russia*
*vshivkov.a@icmm.ru*

M. Narykova, A. Kadomtsev, V. Betechtin
*The Ioffe Institute, 26 Politekhnicheskaya, 194021 St Petersburg, Russia*

**ABSTRACT.** The work is devoted to the study of the damage accumulation in iron under gigacyclic fatigue (VHCF) regime. The study of the mechanical properties of the samples with different state of life time existing was carried out on the base of the acoustic resonance method. The damage accumulation (porosity of the samples) was studied by the hydrostatic weighing method. The obtained results show the accumulation of porosity in the volume of the sample during fatigue loading and corresponding decrease of the elastic properties. A statistical model of damage accumulation was proposed in order to describe the damage accumulation process. The model describes the influence of the sample surface on the location of fatigue crack initiation.

**KEYWORDS.** Gigacycle fatigue; Damage accumulation; Fatigue crack initiation.

## INTRODUCTION

The evolution of structural defects in metals under deformation is observed at all spatial scales and leads to the irreversible deformation and fracture. Nowadays we can observe a rise of interest to study of the defect evolution in metals under VHCF regime [1-12]. The structural investigation of iron tested under HHCF regime was carried out in [13]. One of the key features of a fracture in the VHCF regime is the undersurface fatigue crack initiation. Under this loading condition the crack initiation cannot be detected by a traditional fatigue crack monitoring technique. Due to this fact this regime can be considered as a most dangerous loading regime for real engineering structures.

To develop a model of the defect evolution under small stress amplitude we need to choose the basic physical level of the description of the material microstructure and describe the geometry of the elementary defects. Analysis of the experimental results of the study of structural levels of plastic deformation and fracture and recent experimental investigation can hypothesize that scale level with the size of submicrocracks 0.1-0.3 mm plays a key role in this process [14]. It was experimentally shown that the defect kinetics is different near the specimen surface and within its volume. The rate of the microcrack initiation in the surface layers is from one to three orders of magnitude higher than in the volume of the material.

One of the possible descriptions of defect kinetics is the statistical model of the defect ensemble [15]. This model should take into account the stochastically properties of the defect initiation, their nonlinear interaction and link between micropalsticity and damage accumulation.
This work is devoted to the development of such a model in the application to cyclic loading of metals. To verify the theoretical predictions the experimental study of the defect evolution in iron under VHCF regime was carried out. The experiments were carried out on Shimadzu USF-2000 testing machine. To detect the crack initiation moment an original system was assembled based on the monitoring of magnetic field into the specimen.
For a set of specimens with different degrees of the life time exhaustion an investigation of mechanical properties (elastic modulus, amplitude-independent damping) and the porosity distribution was carried out. The study of mechanical properties was carried out based on the acoustic resonance method using a piezoelectric vibrator with the longitudinal oscillations at frequencies around 100 kHz. The porosity of the specimens was studied by the method of hydrostatic weighing.
As a result, it was shown that the increase of the number of cycles leads to the increase of the porosity of the specimens and to the decrease of their Young's modulus. The porosity of the samples increases from the surface to the axis of the specimen, that confirms the under surface fracture initiation in VHCF regime.

## MATERIAL AND EXPERIMENTAL CONDITIONS

Armco iron samples were used in our investigation. The mechanical properties and chemical composition of the samples are presented in Tabs. 1 and 2.

| C % | Mn % | Si % | S % | P % | Ni % | Cr % | Mo % |
|---|---|---|---|---|---|---|---|
| 0.004 | 0.04 | 0.05 | 0.005 | 0.005 | 0.06 | 0.038 | 0.01 |

Table 1: Chemical composition of iron.

| Young's modulus (GPa) | σ0.2 (MPa) | σb (MPa) | δ (%) |
|---|---|---|---|
| 211.4 | 120-150 | 180-210 | 35 |

Table 2: Mechanical properties of iron.

The geometry of samples is represented in Fig. 1. The structure is presented in Figs. 2.

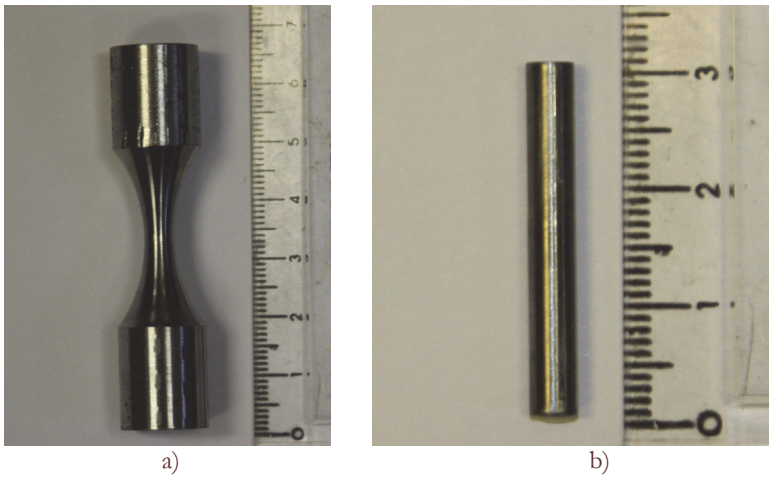

a) b)

Figure 1: Geometry of the samples used in cyclic tests in the VHCF regime (a), geometry of the samples bars with length 30 mm and diameter 5 mm used in acoustic resonance method (b).

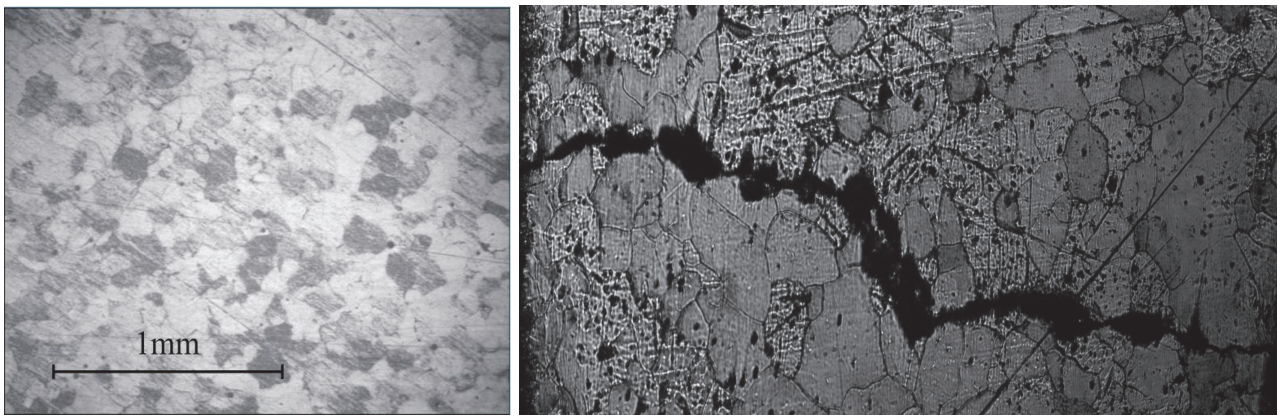


a) b)

Figure 2: Initial structure of the iron sample (a), fatigue crack on the polishing sample surface (b), the depth of polishing 0.15mm.

The fatigue tests were carried out using the Shimadzu USF-2000 ultrasonic testing machine, which provides the accelerated testing of the fatigue properties of materials at 20 kHz. The 20 kHz vibration generated by the piezo element is amplified by the booster and the horn and transmitted to the sample to generate repeated stress. In the ultrasonic fatigue testing system, the vibration system is constructed so that the longitudinal waves transmitted through the solid body are resonating. Consequently, stationary longitudinal waves are formed inside the vibration system (sample, horn and booster). From the physical point of view, the mass of the sample itself plays the role of a generating reactive force, and there is no need to immobilize one side of the sample. The generated strain distribution in the sample can be calculated by the measuring of the displacement of a free side of the sample. The uniform stress testing can be carried out by the controlling of the amplitude of the vibration.
All the samples were tested at the constant stress amplitude up to the failure. The cooling of the sample was realized by an air stream. The temperature of the sample was controlled by the infrared camera. The temperature rise during the experiment is presented in Fig 3.

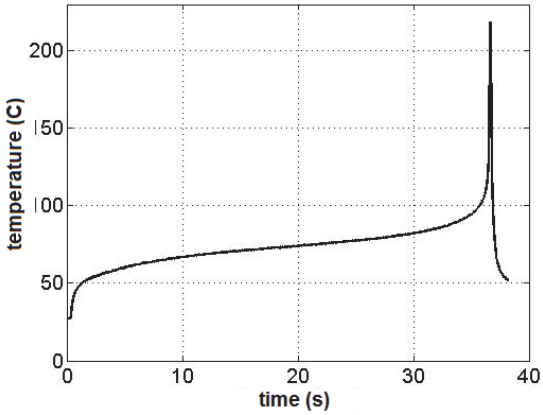


Figure 3: The temperature evolution of the sample during fatigue test.

The Young`s modulus E (a characteristic of elastic properties) and amplitude independent decrement δ (a characteristic of reversible micro plasticity properties) were determined using acoustic resonance method. The main peculiarity of the acoustic experiments is small stress amplitude which doesn't change the dislocation density in the sample.
The measurements were carried out using sectional piezoelectric resonant vibrator. The longitudinal vibrations of samples have a frequency of about 100 KHz. The amplitude was varied in a wide range to investigate both a linear (amplitude-independent) and nonlinear (microplastic) areas.
The essence of the technique is very close to the ultrasonic fatigue test. The sample is connected with piezo element. Stationary acoustic waves are formed inside the vibration system (sample and piezo element). The elastic and micro plasticity characteristics are calculated based of the measurement of a resonant frequency of the system.
Eigen frequency of the longitudinal oscillations $\nu_l$ of bar is connected with Young`s modulus as:

$$\nu_\ell = \frac{n}{2\ell}\sqrt{\frac{E}{\rho}}\left(1-\frac{n^2\pi^2\mu^2 I}{2S\ell^2}\right)$$

where E – Young`s modulus; ϱ – density; *l* – sample length; S – cross sectional area; μ – Poisson's ratio; I – moment of inertia of the sample relative to its longitudinal axis; n – harmonic number.
Eigen frequency of sample can be written as

$$\nu_0 = \nu_2 + \frac{m_1}{m_0}(\nu_2 - \nu_1),$$

where $\nu_1$ – pieze quartz frequency; $\nu_2$ – frequency of the system – piezo quartz and sample; $m_0$ – weight of the sample; $m_1$ – weight of the pieze quartz.
The amplitude independent decrement δ is

$$\delta_0 = \delta_2 + \frac{m_1}{m_0}(\delta_2 - \delta_1).$$

## EXPERIMENTAL RESULTS

The results of ultrasonic fatigue tests are presented in Fig. 4. The scatter and lack of experimental points don't allow us to conclude the duality of Woller-curve and clearly divide the two mechanisms (volumetric and surface) of crack initiation. We can conclude that life time increases with the decrease of the stress amplitude and reaches $10^9$ cycles at the stress amplitude equal to 160 MPa.

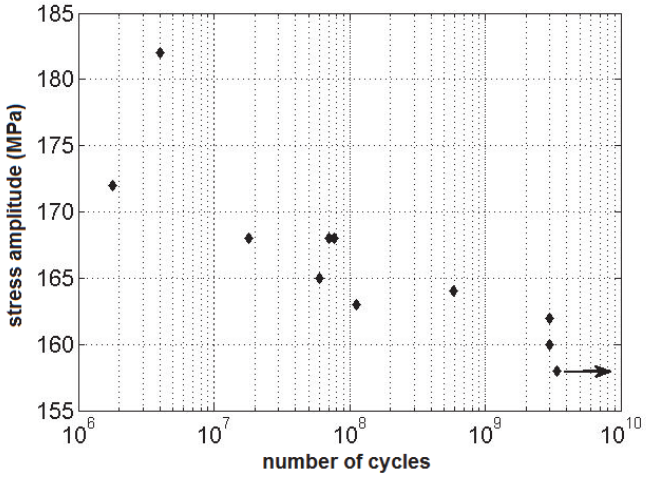


Figure 4: The stress amplitude versus number of cycles to failure under VHCF test.

Five samples with different numbers of loading cycles were chosen for structural investigation: sample 1 (marked П0) is initial state; sample 2 (П1) – $9.01\cdot10^8$ cycles of loading at stress amplitude 161 MPa; sample 3 (П2) – $2.1\cdot10^9$ cycles of loading at stress amplitude 161 MPa; sample 4 (П3) – $3.1\cdot10^9$ cycles of loading at stress amplitude 162 MPa and sample 4 (П4) – cracked (crack is visible to the naked eye) $3.1\cdot10^9$ cycles of loading at stress amplitude 162 MPa. Finally, after preliminary polishing a crack was observed in the sample П3 also. This sample was considered as a fractured also.
The Tab. 3 presents the geometry, weight, density, Young`s modulus and decrement of an iron at different stage of fatigue experiment.
The analysis of data presented in Tab. 3 allows us to conclude that the increase of the number of cycles leads to the decrease of the sample density. It means that the dilatation can be considered as a measure of current damage state of a material. There is a considerable decrease of Young`s modulus with the increase of the number of cycles. Based on the results of previous experiments the decrease of Young`s modulus is linked with the increase of the dislocation density,

microcrack initiation and dilatation. In current situation we can connect the decrease of Young`s modulus from sample П0 to sample П4 with cracks and voids initiation. We can also observe the decreasing of the decrement $\delta_i$ from sample П0 to sample П3 and high increase of the decrement in fully cracked sample П4.

| Sample | d, mm | m, g | ρ, g/cm$^3$ | Δρ/ρ, | E, GPa | δi, $10^{-5}$ |
|---|---|---|---|---|---|---|
| П0 | 5 | 4.65252 | 7.8667 | 0 | 186.2 | 63.0 |
| П1 | 5 | 4.68843 | 7.8654 | $1.6\cdot10^{-4}$ | 184.2 | 52.4 |
| П2 | 5 | 4.63733 | 7.8533 | $1.7\cdot10^{-3}$ | 184.4 | 52.5 |
| П3 | 5 | 4.63920 | 7.8522 | $1.8\cdot10^{-3}$ | 182.5 | 46.5 |
| П4 | 5 | 4.50319 | 7.8522 | $1.8\cdot10^{-3}$ | 169.0 | 890 |

Table 3: Physical and geometrical parameters of iron sample under investigation

Fig. 3 presents the evolution of Young`s modulus as an exponential function of dilatation.

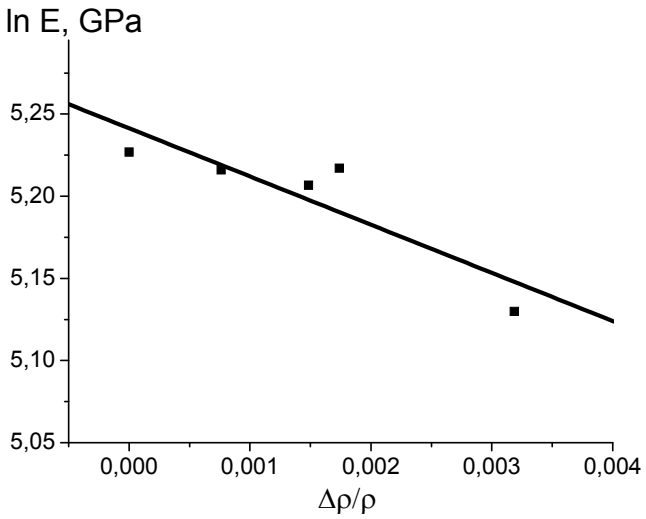


Figure 5: The evolution of Young`s modulus versus dilatation caused by the increase of the number of cycles under fatigue test in VHCF regime.

In order to study the spatial distribution of dilatation as a function of distance from middle cross section of the sample, the sample П 4 is divided into three parts. The central (working) part had the length of 11 mm and weight 1.62199 g. The magnitude of the dilatation of working part with respect to the end (non operative) parts was 0.1%. Symmetrical decrease of the length of the working part to the length of 8 mm leads to the increase of the magnitude up to 0.2%. This result supports a thesis that the maximum of damage accumulation is located in the middle part of the sample and dilatation is distributed in the volume of the specimen.

To study the dilatation distribution along the radius we polished the samples П0-П3 from the radius 5.00 mm to 4.22 mm and measured the density and Young`s modulus after each step of polishing. Tab. 4 summaries the results of this investigation. The density and Young`s modulus of sample П0 are not sensitive to the change of the diameter. The optical microscopy proves the absence of cracks in the samples П0-П2 and existence of cracks in the samples П3, П4 (Fig. 1b). Moreover, the crack opening increases during the polishing. It means that the crack opening is bigger in the volume of the cracked sample.

The data presented in Tab. 4 show that the decrease of diameters leads to the increase of the dilation of the samples П1, П2. Fig. 6 presents evolution of the dilatation of the sample П1 as a function of diameter (Fig 6a) and as a function of the length (fig 6b). The same results were obtained for the sample П2. The cracked sample П3, П4 doesn't exhibit the effect of volume variation of dilatation. It could be caused by the existence of macroscopic crack with the change of the distribution of dilatation.

| Sample | m, g | d, mm | ρ, g/cm$^3$ | E, GPa | δi, 10$^{-5}$ |
|---|---|---|---|---|---|
| П0(initial) | 4.65219 | 5.00 | 7.8787 | 186.2 | 63.0 |
| | 4.68840 | 5.00 | 7.8717 | 184.2 | 52.4 |
| П1 | 4.43544 | 4.90 | 7.8708 | 182.5 | 47.1 |
| | 3.26927 | 4.22 | 7.8686 | 180.0 | 50.9 |
| | 4.63726 | 5.00 | 7.8640 | 184.4 | 52.5 |
| П2 | 4.45456 | 4.90 | 7.8608 | 182.7 | 59.0 |
| | 3.26388 | 4.22 | 7.8602 | 181.7 | 68.4 |
| | 4.63924 | 5.00 | 7.8660 | 182.5 | 46.5 |
| П3 | 4.42786 | 4.90 | 7.8660 | 182.6 | 52.9 |
| | 3.20559 | 4.22 | 7.8660 | 182.4 | 69.0 |
| П4 | 4.50312 | 5.00 | 7.8526 | 169.0 | 890 |

Table 4: Physical and geometrical parameters of samples with different diameters

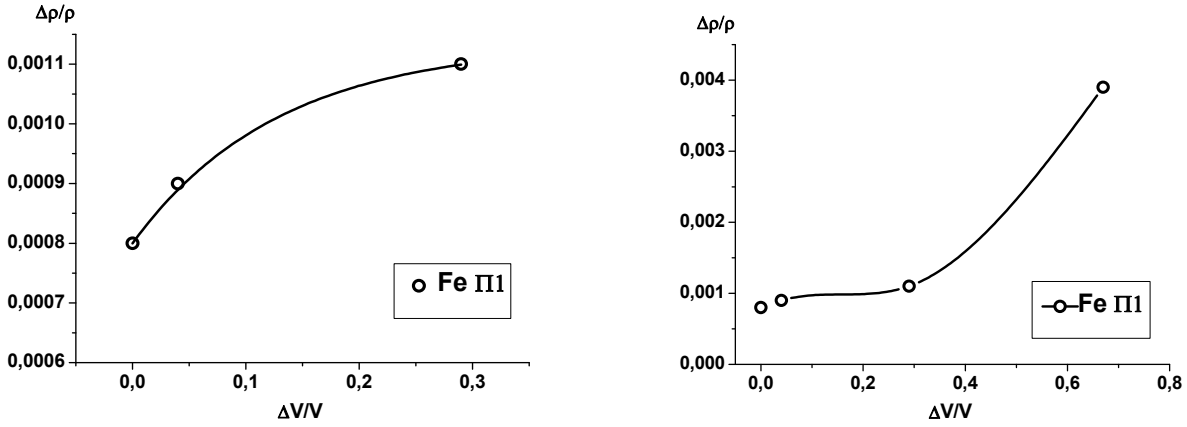


a) b)

Figure 6: The evolution of dilatation Δϱ/ϱ versus variation of sample volume ΔV/V caused by the decrease of the sample diameter (a), the evolution of dilatation Δϱ/ϱ versus variation of sample volume ΔV/V caused by the decrease of the sample length (b).

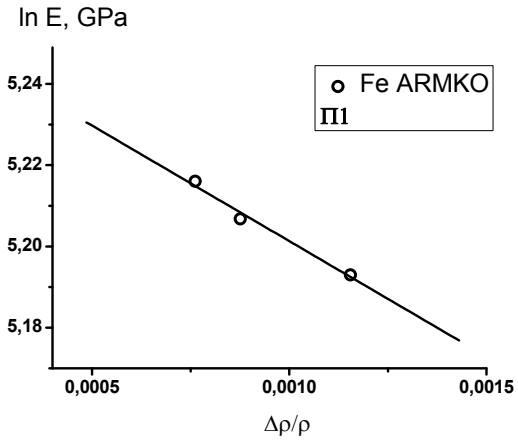


Figure 7: The evolution of Young`s modulus versus dilatation caused by the decrease of the sample diameter.

The Fig. 7 presents the evolution of Young`s modulus of the sample П1 versus dilatation caused by the decrease of the sample diameter. We can observe the expected decrease of Young`s modulus versus dilatation. The evolution of the decrement is not so evident and requests an additional analysis.

## DISCUSSION (SAMPLE SURFACE EFFECT ON LOCATION OF DAMAGE TO FRACTURE TRANSITION POINT)

The experimental results show the important role of dilatation in the failure process under VHCF regime. To describe the evolution of void type defects we can use a statistical approach for the description of the defect evolution proposed in [14]. Under high cycle and VHCF regimes we can assume a weak interaction of defect accumulation and microplastisity processes. Based on Onsager reciprocal relations between defect density rate $\dot{p}$ and corresponding thermodynamic force $\left(\sigma-\frac{\partial F}{\partial p}+\frac{\partial}{\partial x}D\frac{\partial p}{\partial x}\right)$ we can write in one dimensional case

$$\dot{p}=l_p\left(\sigma-\frac{\partial F}{\partial p}+\frac{\partial}{\partial x}D\frac{\partial p}{\partial x}\right), \tag{1}$$

where $l_p$ - Onsager coefficient, $\sigma$ - applied stress, $F$ - part of free energy of the system which depends on $p$ only, $D$ - the coefficient of self-diffusion which is known to obey the Arrenius law, $D=D_0\exp\left(-E_{sd}/T\right)$ ($E_{sd}$ is the activation energy of self-diffusion) and largely depends on the defect concentration.
In order to illustrate the effect of the sample surface we consider two representative material volumes $V_{sur}$, $V_{bulk}$ located near the specimen surface (part of the surface volume coincides with the specimen surface) and into specimen volume, respectively. If we introduce a mean strain induced by the defect initiation in the considering volume as $p_m=\frac{1}{v_i}\int_{v_i}p dv$ we can rewrite the Eq. (1) as

$$\dot{p}_m+\frac{h\,l_p}{V}p_m=l_p\left(\sigma-\frac{\partial F}{\partial p}\right)_m, \tag{2}$$

where we used the following boundary conditions

$$D\frac{\partial p}{\partial x}\bigg|_{p\in S}=-\frac{h}{V}\int_{v_i}p dv\,. \tag{3}$$

The Eq. (3) requests an approximation of $\sigma-\frac{\partial F}{\partial p}$ function which determined the equilibrium states of material with defects. Taking into account the solution of statistical problem of defect evolution [2] we can propose the following approximation for defect evolution law

$$\dot{p}_m+\frac{h\,l_p}{V}p_m=l_p\left(\frac{n\sigma^2}{n_0E^2}\left(p_m+p_0\right)^2-a\,p_m\right), \tag{4}$$

where $n$ is initial defect concentration, $\sigma$ is the mean stress for the considered volume, $p_0, l_p, a$ are material constants, $h$ -the constant which determines the boundary conditions for considered volumes.
To explain the different mechanisms of crack initiation on specimen surface and in volume we need to consider a surface as a physical object with high concentration of incomplete atomic planes and other defects of different nature.

As a result we can consider the surface as negative source with infinite capacity which has a great influence on the defect evolution. This influence can be described by the value of constant $h$ in the boundary condition (4).
There are two limiting cases for Eq. (4). The first case is $h \to \infty \Rightarrow p\big|_{p\in S} = 0$. It means the surface is the sink of infinite capacity and this condition can be used for the description of defect evolution close to specimen surface ($V_{sur}$). The second case is $h \to 0 \Rightarrow D\dfrac{\partial p}{\partial x}\Big|_{p\in S} = 0$. The surface is closed for the defect diffusion. This condition can be used for the description of the defect evolution in the volume of the specimen ($V_{bulk}$).
Let us introduce the following dimensionless variables $\tau = t\,l_p a$, $n' = n / n_0$, $\Psi = \sigma / (Ea)$, $h' = h / (V a)$, taking into account the fact that the initial defect (submicrocrack) concentration near specimen surface is one or two order higher than in the volume of the specimen ($n'_{sur} >> n'_{bulk}$) and there is the difference in boundary conditions, we can write the Eq. (4) for $V_{sur}$, $V_{bulk}$ as

$$\dot{p}_m = n'_{sur}\Psi^2\left(p_m + p_0\right)^2 - \left(1 + h'\right)p_m, \tag{5}$$

$$\dot{p}_m = n'_{bulk}\Psi^2\left(p_m + p_0\right)^2 - p_m. \tag{6}$$

Under one dimension loading the stress is equal for both representative volumes and can be written as $\Psi = \Psi_0\cos(\omega\tau)$. The numerical solutions of Eqs. (5,6) are presented in Fig. 8.

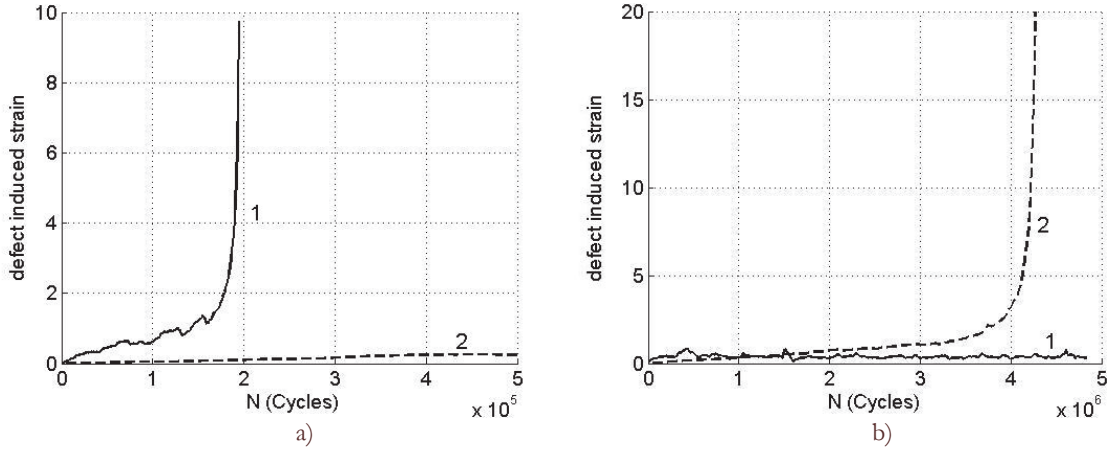


Figure 8: Defect induced strain evolution near specimen surface (1) and in the volume of the specimen (2) for high (a) and small stress amplitudes (b).

At high stress amplitude the initial defect concentration plays the main role and leads to the sharp increase of the defect density near specimen surface (Fig.8a). The blow-up regime of defect accumulation can be considered as damage to fracture transition and can manifest the emergence of macroscopic crack. At small stress amplitude the defect diffusion and defect annihilation on specimen surface lead to the low defect growth near specimen surface and blow-up regime of defect accumulation can be observed in the volume of the specimen (Fig. 8b).
In the case of proposed approximation the critical time in the Eq. (6) can be estimated as follows

$$t_f = \int_0^{\infty} \frac{\left(1 + h'\right)p_m}{n'_{sur}\Psi^b\left(p_m + p_0\right)^b}dp. \tag{7}$$

To describe the full S-N curve we have to use several Eqs. (5) with different values $h', n'$ which could be connected with initial heterogeneity of materials. The Eq. (6) gives the traditional representation of S-N curve in Basquin form

$$\ln\left(N_f\right) = a - b\ln\left(\Psi\right), \tag{8}$$

where $a = \nu \int_0^{\infty} \frac{\left(1+h'\right) p_m}{n'_{sur}\left(p_m + p_0\right)^b} dp$, $\nu$ is a loading frequency.

## Conclusion

Summing up the results of structural investigation of iron samples we can make several conclusions.
The increase of the number of cycles leads to the dilatation of iron samples. The dilatation can be caused by initiation of new dislocations, micro voids and cracks. The hydrostatic weighing shows that the maximum of dilatation is observed in the middle part of the sample.
The decrease of diameters of samples П1, П2 show the decrease of Young`s modulus and dilatation. The crack in the sample П3 doesn't allow us to find the change in the dilation and elastic properties. The observed dilatation in the samples П1 и П2 shows the initial stages of micro voids and micro cracks formation in the volume of the sample and initiation of crack under surface. The investigation of crack opening evolution and elastic properties of the samples also supports these results.
The small size and high concentration of microvoids and microcracks allow us to propose a statistical description of microcrack evolution in metals under cyclic loading and introduce a new thermodynamic variable – defect induced strain. The new variable gives a natural description of thermodynamics of metals with microcracks and allows us to describe the interaction of plasticity and failure processes. This model coupled with a description of nonlocal effect in the defect ensemble. This gives us a key parameter for the description of defect kinetics in the volume of the sample and near its surface under cyclic loading.
Based on the developed model the new equation for defect kinetics in the volume of the specimen and near its surface has been proposed. The surface was considered as a physical object with high concentration of incomplete atomic planes and other defects of different nature. It allows us to explain the difference in the defect kinetics far and close to the specimen surface and describe the damage to fracture transition both in the volume of the specimen and near its surface.
It was shown that the stress amplitude can influence on the location of macro fatigue crack initiation. At small stress amplitude the defect induced strain reaches an equilibrium value near specimen surface due to the defect diffusion and annihilation processes. It can be considered as an infinite fatigue life but in this case there is possibility of blow-up regime of defect kinetics in the volume of the specimen. It leads to the shift of the location of the crack initiation from the surface to the volume of the specimen.
The developed theoretical model describes the important role of the specimen surface and its physical state in the process of the defect accumulation under cyclic loading. This model proposes a physical mechanism of the shift of the crack initiation location from the specimen surface to its volume that experimentally observed under VHCF regime (cyclic loading with small stress amplitude). It is interesting to note that the best experimental verification of the model could be carried out on the base of the structural investigation of microcrack accumulation in the fine grain metals (materials with high concentration of initial submicrocracks) under VHCF regime.

## Acknowledgments

The work was supported by the Ministry of education and science of the Russian Federation (contract No 02.G25.31.0068 of 23.05.2013 as part of measures for implementation of the Presidential decree of the Russian Federation government No 218).

## References

[1] Zhu, X., Shyam, A., Jones, J.W., Mayer, H., Lasecki, J.V., Allison, J.E., Effect of microstructure and temperature on fatigue behavior of E319-T7 cast aluminum alloy in very long life cycles, Int. J. Fatigue, 28 (2006) 1566-1571.
[2] Bathias, C., Paris P., Gigacycle Fatigue in Mechanical Practice, Taylor & Francis, (2004) 328.

[3] Botvina, L.R., Gigacyclic fatigue – a new problem of physics and mechanics of fracture, Zavodskaya laboratoria, 70 (2004) 41.
[4] Shaniavski, A.A., Skvortsov, G.V., Crack growth in the gigacycle fatigue regime for helicopter gears, Fatigue & Fracture of Engineering Materials & Structures, 22 (1999) 609-619.
[5] Sakai, T., Review and prospects for current studies on very high cycle fatigue of metallic materials for machine structural use, Journal of solid mechanics and materials engineering, 3 (2009) N 3 425-439.
[6] Wang, Q.Y., Berard, J.Y., Rathery, S., Bathias, C., High cyclic fatigue carack initiation and propagation behavior of high strength spring steel wires, Fatigue & Fracture of Engineering Materials & Structures, 22 (1999) 673-677.
[7] Sun, C., Xie, J., Zhao, A., Lei, Z., Hong, Y., A cumulative damage model for fatigue life estimation of high-strength steels in high-cycle and very-high-cycle fatigue regime, Fatigue &Fracture of Engineering Materials & Structures, 5 (2012) 638-647.
[8] Shiozawa, K., Morii, Y., Nishino, S., Lu, L., Subsurface crack initiation and propagation mechanisms in high strength steel in a very high cyclic fatigue regime, Int. J. Fatigue, 28 (2006) 1521-1532.
[9] Tanaka, K., Akiniwa, Y., Fatigue crack propagation behaviour derived from S–N data in very high cycle regime, Fatigue Fract. Eng. Mater. Struct, 25 (2002) 775–784.
[10] Wang, Q. Y., Bathias, C., Kawagoishi, N., Chen, Q., Effect of inclusion on subsurface crack initiation and gigacycle fatigue strength, Int. J. Fatigue 24 (2002) 1269–1274.
[11] Tanaka, K., Mura, T., A dislocation model for fatigue crack initiation, J. Appl. Mech, 48 (1981) 97–103.
[12] Chapetti, M. D., Tagawa, T., Miyata, T., Ultra-long cycle fatigue of high-strength carbon steels part II: Estimation of fatigue limit for failure from internal inclusions, Mater. Sci. Eng., 356 ( 2003) 236–244.
[13] Wang, C., Wagner, D., Wang, Q.Y., Bathias, C., Gigacycle fatigue initiation mechanism in Armco iron. International Journal of Fatigue, 45 (2012) 91-97.
[14] Betekhtin, V. I., Kadomtsev, A. G., Evolution of microscopic cracks and pores in solids under loading. Physics of the solid state, 47 (2005) 825–831.
[15] Plekhov, O. A., Naimark, O. B., Theoretical and experimental study of energy dissipation in the course of strain localization in iron Journal of Applied Mechanics and Technical Physics, 50 (2009) 127-136.